

Luminescence studies of blue-green $\text{BaAl}_x\text{O}_y:\text{Eu}^{2+},\text{Dy}^{3+}$ nanophosphors synthesized using solution-combustion method

M Abshiro¹ and FB Dejene^{1*}

*Department of Physics, University of the Free State (QwaQwa campus, Private Bag X13, Phuthaditjhaba, 9866, South Africa)

*Corresponding author. Tel: +27587185263, fax: +27587185444

e-mail address: dejenebf@qwa.ufs.ac.za

Abstract

Blue-green luminescent $\text{BaAl}_2\text{O}_4:\text{Eu}^{2+},\text{Dy}^{3+}$ phosphor powders were synthesized using the solution combustion method. The effects of preparation conditions such the variation of amount of urea and the addition of boric acid as flux on the structural and luminescence properties of the powders were investigated. The phosphors were characterized by X-ray diffraction (XRD), scanning electron microscopy (SEM) and fluorescence spectrophotometer. In the combustion reaction process, the contents of urea determine the adiabatic temperature of combustion and the reaction sustainability which both influence the formation of BaAl_2O_4 phase and photoluminescence properties. So, we investigated the boric acid content on the host phase, and prepared some samples with poor-fuel, stoichiometric, rich fuel and with or without boric acid.

Keywords: $\text{BaAl}_2\text{O}_4:\text{Eu}^{2+},\text{Dy}^{3+}$, Nanophosphors, Solution-combustion, Structure, Luminescence

1. Introduction

Aluminate phosphors are emission efficient, chemically and thermally stable oxides. They are popularly used as high loading fluorescent lamps for general lighting purposes. Most of the aluminate phosphors are activated by rare-earth ions and require high temperature firing for synthesis. The $\text{BaAl}_2\text{O}_4:\text{Eu},\text{Dy}$ crystal structure can be classified into five types according to the lattice site where the Ba^{2+} ion is located and the different of the stacking of the spinel lattice and the Ba^{2+} -containing layers. The Ba^{2+} ion enters into different lattice sites depending on the small differences in the matrix composition. As the Eu^{2+} activator substitutes into Ba^{2+} sites, its emission spectrum is affected by the matrix elements as well. The replacement of Ba^{2+} (ionic radius = 1.33 Å) by Eu^{2+} (ionic radius = 1.13 Å) induces a change in the crystal field which might shift the emission peaks depending on the $\text{Eu}^{2+}:\text{Ba}^{2+}$ mole ratio. The $\text{BaAl}_2\text{O}_4:\text{Eu},\text{Dy}$ phosphors is generally characterized with one strong and broad emission peak at about 450 nm. This is attributed to the characteristic $4f^7 \rightarrow 5d^1$ transition of Eu^{2+} ions. In order to enhance the luminous properties, many researchers have studied these phosphors by varying the concentration of europium [1], different charge compensators [2,3], and different synthesis methods [4-7]. The conventional solid-state reaction for preparing long afterglow phosphors requires a high calcining temperature, which induces sintering and aggregation of particles. Furthermore, the milling process to reduce the particle size leads to decreasing of luminescence properties [8]. The processing routines used during synthesis of phosphors by sol-gel techniques, are also complicated and the duration is long. The solution-combustion method to synthesize the phosphors, however, can produce a homogenous product in a short time without the use of expensive high-temperature furnaces [9-11]. This synthesis technique makes use of the heat energy liberated by the redox exothermic reaction at relative low igniting temperature between metal nitrates and urea or other fuels [12]. Furthermore, the process is very facile and energy saving. The mechanism of the combustion reaction is quiet complex. The parameters that influence the reaction include: type of fuel, fuel to oxidizer ratio, use of excess oxidizer, ignition temperature, and water content of the precursor mixture [13]. In this work, the $\text{BaAl}_2\text{O}_4:\text{Eu},\text{Dy}$ nano phosphors were synthesised by the solutions-

combustion method using urea as a fuel and boric acid as a flux agent. The influence of the mol ratio of boric acid flux to barium nitrate and the initiating temperature on the luminescent properties of the $\text{BaAl}_2\text{O}_4:\text{Eu},\text{Dy}$ phosphors were investigated.

2. Experimental procedure

$\text{BaAl}_x\text{O}_y:\text{Eu}^{2+},\text{Dy}^{3+}$ phosphor powders were prepared by the solutions combustion method using boric acid as flux material. To investigate the effect of different amount of boric acid on the structural and PL properties of the $\text{BaAl}_x\text{O}_y:\text{Eu}^{2+},\text{Dy}^{3+}$ phosphor, samples with different mole % of the flux were prepared under atmospheric pressure without post treatment. The solutions were prepared by dissolving various amounts of the nitrate precursors of each component into distilled water. The resulting solution was transferred into a crucible, which was then introduced into a muffle furnace maintained at 500°C for 5-6 minutes. The voluminous and foamy combustion ash was easily milled to obtain the final $\text{BaAl}_x\text{O}_y:\text{Eu}^{2+},\text{Dy}^{3+}$ phosphor powder. XRD patterns of the as-synthesized samples were recorded on an x-ray diffractometer with $\text{Cu K}\alpha = 1.5406 \text{ \AA}$, which was operated at 40 kV voltage and 40 mA anode current. Data were collected in 2θ values from 20° to 80° . The morphologies and size of particles were examined using a PHI 700 Nanoprobe and a Shimadzu model ZU SSX – 550 Superscan scanning electron microscope (SEM), coupled with an energy dispersive x-ray spectrometer (EDS). Photoluminescence measurement was performed at room temperature on a Cary Eclipse fluorescence spectrophotometer (Model: LS 55) with a built-in 150 W xenon lamp as the excitation source and a grating to select a suitable wavelength for excitation.

3. Results and discussions

3.1 Morphological and structural properties

The representative SEM micrograph of samples prepared without boric acid and with 10 % boric acid is shown in Fig. 1. It is observed that the sample without B_2O_3 addition revealed mixture of rod like and granular nanostructure and that the surface of the powder samples showed lots of voids and pores. The presence of the B_2O_3 content, by gradually increasing the particle size and the morphology became agglomerative.

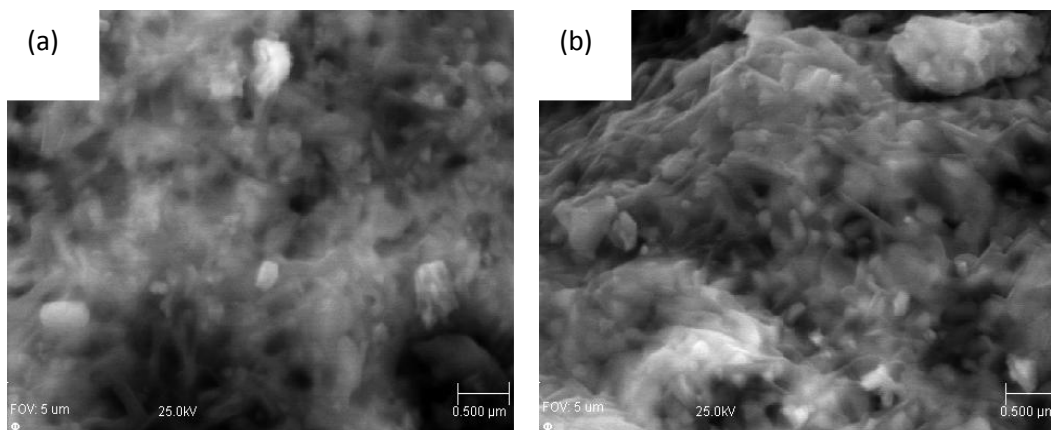


Fig. 1 SEM micrographs of as-synthesized $\text{BaAl}_x\text{O}_y:\text{Eu}^{2+},\text{Dy}^{3+}$ (a) without boric acid depict mixture of rod like and granular nanostructure and (b) 10 % boric acid.

The samples with 15 mol% B_2O_3 acid content resulted into irregular morphologies with heavily agglomerated particles. It is suggested that higher B_2O_3 content can lead to more borate flux to carry out

the dissolution–precipitation process for the formation of BaAl_2O_4 , thereby enhancing the agglomeration of resultant particles. The EDS measurements confirm the presence of the Ba, Al, O, Eu and Dy.

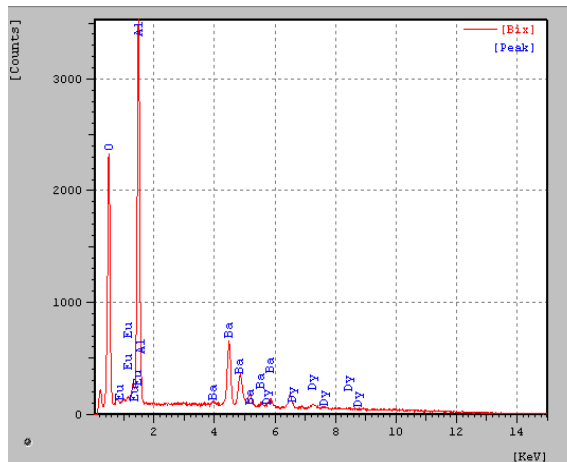


Fig. 2 The corresponding EDX analysis confirming the existence of all elements involved in phosphor preparation

Fig. 3 shows the XRD patterns of the four phosphor powders prepared using various amount of boric acid. As shown in Fig. 3, the dominant crystal phase of the product for samples without boric acid was hexagonal BaAl_2O_4 structure. However, there was a little impurity in the product. In spite, the peaks of product were far more intensive and sharper than those of samples with boric acid, so it was believed that the crystals in powders much better crystallized. The XRD results revealed changes in structure from hexagonal BaAl_2O_4 to a tetragonal $\text{Ba}_{17}\text{Al}_3\text{O}_7$ phase as the boric acid content increased from 0 to 15%. According to the Scherrer formula, the average crystallite size of the powders for samples without boric acid and that with 7 mol % was calculated as 39.2 and 53.1 nm, respectively, which was mainly associated with the combustion temperature reached during combustion process. The combustion temperature of product with boric acid were much higher than that of precursors without boric acid, as a result, the former exhibited a larger average crystallite size.

3.2 Optical properties

Fig. 4 (a) and (b) reveal the effect of boric acid flux on the photoluminescence properties of $\text{BaAl}_2\text{O}_4:\text{Eu}^{2+},\text{Dy}^{3+}$ phosphor particles prepared by solution-combustion method. The excitation spectrum of phosphors generally show a broad-band spectrum extending from 250 to 400 nm where the position of the maximum intensity wavelength shifts from low to high edge with the boric acid content. The sample prepared from the precursor mixture without boric acid flux had highest or strong excitation intensity. The emission spectra prepared from precursor mixture without boric acid flux exhibits symmetrical blue-green broad peak at about 505nm which is attributed to the typical transition between the ground state ($4f^7$) and the excited state ($4f^6 5d^1$) of Eu^{2+} ions. It has been reported the emission spectrum of the $\text{BaAl}_2\text{O}_4:\text{Eu}^{2+},\text{Dy}^{3+}$ samples obtained by solid state method presented a main peak at 500 nm, and a shoulder peak at 435 nm. Compared to our results, it clearly exhibited a slight blue shift of the broad band which might be caused by the quantum size effect [2, B]. Sample with boric acid show peaks at 480, 580, 615 and 656 nm. The samples with 15 mol% B_2O_3 acid content significantly quench the luminescence phenomenon. The presence of boric acid was observed to completely reduce the intensity of blue emission (505nm) while enhancing an emission at 480 nm and the red emissions. When the molar ratio of boric acid was 15mol%, the phosphor particles prepared from the precursor mixture exhibited the maximum photoluminescence intensity. Therefore, it can be concluded that H_3BO_3 did not only act as an inert high

temperature solvent medium (flux); it actively participated in reactions and depending upon the amount of H_3BO_3 . It was summarised from the PL results that variation peak position with the presence of boric acid can be attributed to the change of crystalline phase, which are in good agreement with the XRD data. The decay curve of samples synthesized with different content of boric acid is shown in Fig. 5. The samples prepared from precursor mixture without boric acid flux exhibits the shortest afterglow and the highest initial intensity, which was in accordance with the photoluminescence intensity of the samples. The decay characteristics show that the afterglow property was enhanced by the addition of B_2O_3 [3] up to 7 mol % and thereafter reduces phosphorescence property. The B_2O_3 acts as an inert high temperature solvent (flux) to facilitate the grain growth of barium aluminates. These increase the penetration of trap centers in the ceramics and therefore achieve improvements in persistence luminescence.

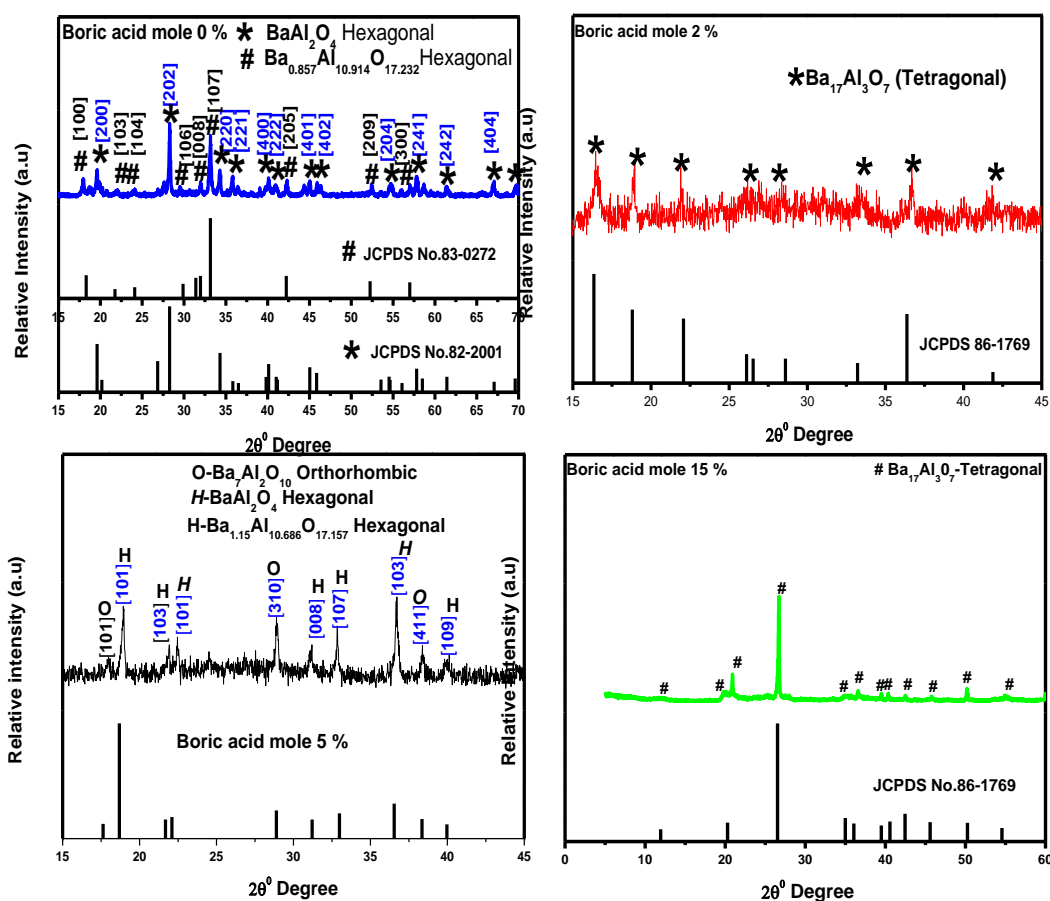


Fig. 3 XRD patterns of the solution-combustion synthesized phosphors powders using (a) 0% (b) 2% (c) 5% and (d) 15% citric acid as a flux.

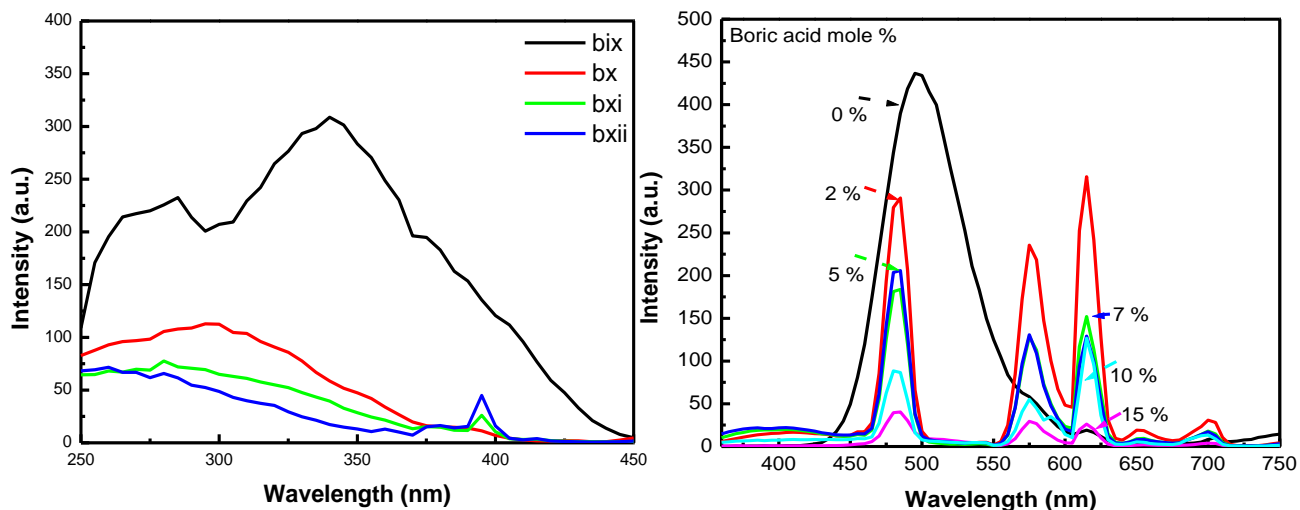


Fig. 4 PL emission spectra ($\lambda_{exc}=325$ nm) of $BaAl_xO_y:Eu^{2+},Dy^{3+}$ phosphor for different content of boric acid

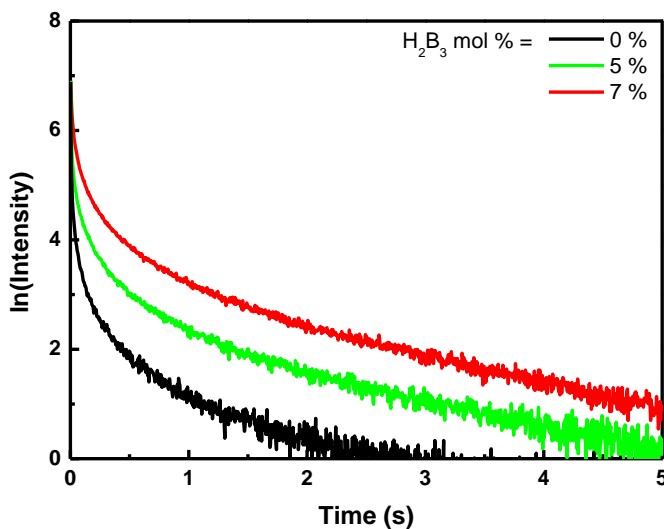


Fig. 5 Lasting time of phosphorescence from $BaAl_2O_4:Eu^{2+},Dy^{3+}$ corresponding to phosphor powders with different content of boric acid.

4. Conclusion

The $BaAl_2O_4:Eu^{2+},Dy^{3+}$ phosphor with varying amount of boric acid was successfully synthesized by solution combustion method. The $BaAl_2O_4:Eu^{2+},Dy^{3+}$ phosphor particles are irregularly in shape and aggregated with an average particle size of 35–60 nm. The main diffraction peaks index well with the

hexagonal crystalline phase. PL characteristics and decay time investigated for varying samples also show that the sample with 7 mol % had the highest PL intensity and longer afterglow for blue-green emission. The position of the emission peak in blue domain does change with the presence of boric acid due to change in crystalline structure. Thus, the luminescent center ions and the density of traps become large with the presence of flux, which make the afterglow properties better.

Acknowledgement

The financial support of the National Research Foundation (NRF) and the University of Free State are acknowledged.

References

- [1]. Chen X Y, Ma C, Li X X, Shi C W, Li X L and Lu D R 2009 *J. Phys. Chem. C*, 113 2685.
- [2]. Stefani R, Rodrigues L C V, Carvalho C A A, Felinto M C F C, Brito H F, Lastusaari M, Hölsä 2009 *Journal of Optical Materials*, 31(12): 1815.
- [3]. Diallo P T, Jeanlouis K, Boutinaud P, Mahiou R, Cousseins J C, 2001 *J. Alloys Compd.* 323/324 218–222.
- [4]. Nag A and Kutty T R N 2004 *Mater. Res. Bull.* 39 331.
- [5]. Blasse G and Grabmaier B C, in “Luminescent Materials” (Springer-Verlag, Berlin, 1994) p.33.
- [6]. Lu Y Q, Li Y X, Xiong Y H, Wang D and Yin Q R 2004 *Microelectron. J.* 35 379.
- [7]. Aruna S T and Mukasyan A S 2008 *Curr. Opin. Solid ST. M.*, 12 44.
- [8]. Patil K C, Aruna S T and Mimani T 2002 *Curr. Opin. Solid ST. M.*, 6 507.
- [9]. Ianos R and Lazau I 2009 *Mater. Chem. Phys.*, 115 645.
- [10]. Rao R P 1996 *J. Electrochem. Soc.* 143 189.
- [11]. Peng T Y, Yang H P, Pu X L, Hu B, Jiang Z C and Yan C H 2004 *Mater. Lett.* 58 352–356.
- [12]. McKittrick J, Shea L E, Bacalski C F and Bosze E J 1999 *Displays* 19 169–172.